

Research

Vortex induced flower-like Ni-Co coating by a hydrothermal approach**Yong Zhang***, Fang LiuSchool of Materials Science and Engineering, Dalian Jiaotong University,
Dalian 116028, China**Received date:** 28-03-2016; **Accepted date:** 26-04-2016; **Published date:** 29-04-2016**CORRESPONDENCE AUTHOR:** Yong Zhang**Tel.:** +86-0411-84105850; **E-mail:** zhangyong0411@126.com**CONFLICTS OF INTEREST**

There are no conflicts of interest for any of the authors.

ABSTRACT:

Flower-like Ni-Co coating was deposited on copper substrate by a hydrothermal approach. Detailed experimental result revealed that, the achieved Ni-Co coating exhibited flower-like morphology. During sliding wear tests, the volume loss of Ni-Co coating was 20.4 % of copper substrate, obviously increasing the wear properties of copper substrate. During hydrothermal reactions, convective flows existed. Moreover, water jets were produced by bubble collapse. Interaction of convective flows and water jets resulted in vortex flows. Driven by the flowing force of helical vortex, Ni and Co plates were assembled to flower-like Ni-Co architectures.

Key words: Hydrothermal; Flower-like; Vortex; Bubble; Ni-Co coating**1. INTRODUCTION**

Vortex, the fascinating natural phenomenon has aroused numerous attentions in scientific research. Vortex generator [1] and vortex diode [2] have been reported. Moreover, large vortices were achieved from soap bubbles by Kellay et al [3]. Hermans et al. [4] investigated the chirality-specific lift forces imported by vortex flows, which exhibited promising applications in separation technologies.

Vortex is formed by rotated flows. Owing to the ideal helical shape of vortex, helical flows of vortex are achieved. These vortex flows exhibit promising applications to drive the helical assembly of three-dimensional structures. However, vortex induced self-assembly of unique morphological micro/nano-architectures has rarely been found, to the best of our knowledge.

Convection [5] exists during hydrothermal reactions. Furthermore, bubbles are created in the boiling hydrothermal solution [6], and water jets are produced by bubble collapse [7]. Induced by the water jets, rotation of convective flows may occur in local regions of autoclave, resulting in vortex flows. Inspired by this idea, we deposited flower-like Ni-Co coating on copper substrate by means of hydrothermal approach, in which the growth mechanism of flower-like Ni-Co architectures was investigated. The vortex assembly approach will

provide some new insights for the controllable growth of micro/nanostructures.

2. EXPERIMENTAL

Specimens with dimensions of 10×5×15 mm³, cut from pure copper plates (Cu: Cr = 99.9: 0.1), were used as substrates. Then, the copper samples were pre-treated by H₂SO₄, HCl solution and sandblast treatment. In a typical experiment, citric acid (C₆H₈O₇·H₂O), CoCl₂·6H₂O and NiCl₂·6H₂O were successively dissolved in 70 mL of deionized water. Then, NaH₂PO₂·H₂O was added, in which the pH value of resulting solution was about 5~6. After stirring for 30 minutes at room temperature, the resulting solution was loaded in a 100 mL Teflon-lined autoclave and hydrothermally treated at 110 °C for 2 h. Finally, the samples were treated at 973 K for 1 h under argon atmosphere.

The morphology of reaction products was observed by scanning electron microscopy (SEM, JSM-6360LV) and high resolution transmission electron microscopy (HRTEM, JEOL2010F). The crystallographic characterization was performed by an X-ray diffraction (XRD, D/Max-Ultima⁺, with an accelerating voltage of 40 kV) with Cu Ka radiation at a scan speed of 6 °/min.

The surface microhardness of the samples was measured using FM-700 Vickers microhardness

instrument at a load of 100 g for a loading time of 15 seconds. Rhombic diamond indenter was used in our experiment, with three indentations for each load, and the other parameter were adopted according to ASTM E384-08.

In reference of previous work [8], unlubricated sliding wear tests were conducted with pin-on-disk apparatus (SFT-ZM tester, Materials Tester Company, Xuanhua, Hebei Province, China) under dry sliding conditions at room temperature, in which copper substrate cylinders, Ni-Co coatings coated copper cylindrical samples of $\Phi 5$ mm \times 18 mm dimensions were used as the pins, respectively, with the GCr15 sliding disk of 60 HRC hardness and 30 mm in diameter used as counter-body. During sliding wear tests, the applied load was 8 N. A fixed rotating speed of 200 rpm was used and each test was performed for 10, 20, 30 and 60 minutes, respectively. The surface of wear tests samples was ground and polished with 2000 # grit paper. According to the ASTM G99-95a standard, the volume loss was calculated from the pin height change under wear testing, and more than three times replicate wear experiments were performed.

3. RESULTS AND DISCUSSION

3.1 Microstructure of the coatings

SEM observation of the as-synthesized coating is shown in Fig. 1. Abundant aggregated microstructures are achieved (Fig. 1(a)). Mostly, they are flower-like products. Several spherical particles are found, with micro-pores existing in the spherical particles (Fig. 1(b) and (c)). In addition, the flower-like products are assembled by plate-like crystals (Fig. 1(d) and (e)).

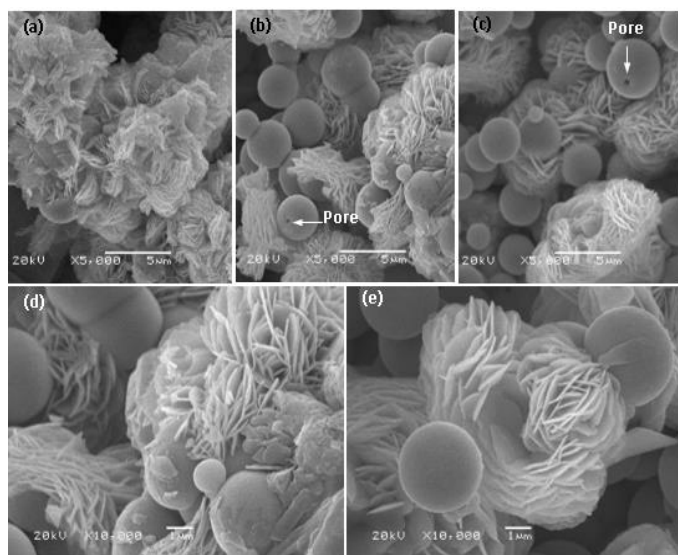


Fig. 1: Surface SEM morphologies of the as-synthesized coating on copper substrate.

Interestingly, the plate-like crystals are helically arranged in the flower-like products (Fig. 2(a)). In the core region of flower-like products, the plate-like crystals are radially distributed (Fig. 2(b)). High-magnification SEM observation reveals that, the plate-like crystals are composed of even smaller plates with 10~20 nm thickness (Fig. 2(c) and (d)). Helical assembly of plate-like crystals around spherical particles is also found, and several micro-pores exist in the spherical particles and plate-like crystals (Fig. 2(e) and (f)). Moreover, much more micro-pores are found near the spherical particles and flower-like products (Fig. 2(g)), in which the plate-like crystals are helically assembled (Fig. 2(h)).

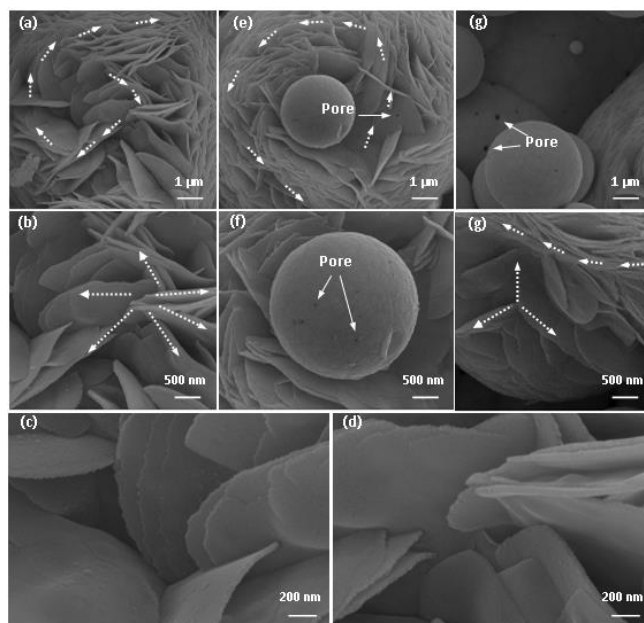


Fig. 2: High-magnification surface SEM observation of the as-synthesized coating.

XRD pattern of the as-synthesized coating is shown in Fig. 3. The strong peak at 44.0° is resulted from Ni(111) (JCPDS card, 65-0380) and Co(002) (JCPDS card, 89-4308) planes, revealing the as-synthesized coating is Ni-Co coating. Moreover, the peaks at 47.6° and 51.8° are corresponded to Co(101) and Ni(200) planes, respectively, indicating the preferred growth of Ni and Co plates in Ni-Co coating. Additionally, NiP (JCPDF Card, 74-1382) and CoP (JCPDF Card, 89-2747) are also formed in the Ni-Co coating.

Fig. 4 is HRTEM observation of the Ni-Co coating. Plate-like structures with 20~30 nm thickness are found (Fig. 4(a) and (b)). The selected area diffraction pattern demonstrates that, Ni(111) and Ni(220) are the preferred growth planes of Ni plates (inset of Fig. 4(b)). The inter planar spacing's of plate-like crystal are about 0.20 nm and 0.13 nm, respectively (Fig. 4(c), (c₁) and (c₂)), corresponding

to Ni(111) and Ni(220) planes, respectively. This result confirms the preferred growth of Ni plates. Moreover, plate-like crystal which exhibits the fringe of Co(002) plane with an inter planar spacing of about 0.20 nm is found (Fig. 4(d)), confirming the preferred growth of Co plates.

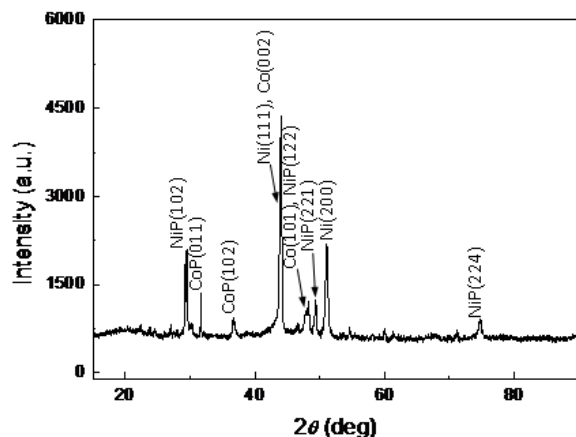


Fig. 3: XRD pattern of the as-synthesized coating.

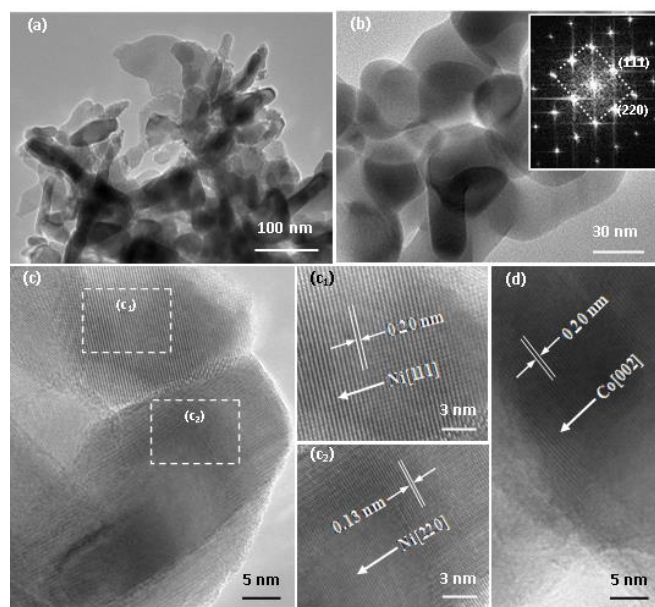
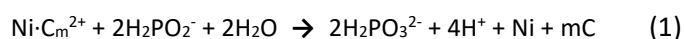


Fig. 4: HRTEM characterization of the as-synthesized Ni-Co coating.

3.2 Growth Mechanism of Flower-like Ni-Co Coating

In reference of our previous report [9], hydrothermal growth of Ni-Co coating can be described as following:



Where, Ni·C_m²⁺ and Co·C_m²⁺ are the complexing compound obtained from complexing reaction of Ni²⁺, Co²⁺ and complexing agent C_m (such as citric acid, lactic acid, etc.), in which formation of Ni·C_m²⁺ and Co·C_m²⁺ prevents the precipitation of Ni(OH)₂ and Co(OH)₂ sediment.

Usually, nanostructures are grown along some low index crystal planes such as {111}, {100} and {110}, to fulfill the smallest surface energy principle [10]. For this reason, preferred growth of Ni atoms along Ni(111) plane results in plate-like structures. Similarly, Co plates are achieved by preferred growth of Co atoms along Co(002) plane.

Flower-like assembly of Ni-Co architectures is related to the helical flows of vortex during hydrothermal reactions. Due to the temperature difference between bottom and upper regions of autoclave, natural convection appears [10]. Convective flows are produced in the autoclave, as demonstrated in Fig. 5(a). Moreover, bubbles are produced in the boiling water solution of hydrothermal reactions. With the increasing of inner pressure of autoclave, bubble collapse occurs, and water jets are produced (Fig. 5(b)). A resultant force F of Ni and Co plates in hydrothermal solution is achieved, by the combination of convective floating force F₁ and water jet force F₂. Compared with the original F₁ flow direction, the resultant F flow direction rotates certain degree (Fig. 5(c)).

Bubbles continuously appear and float from the bottom to the upper surface of hydrothermal solution, and bubble collapse reactions continuously happen. Rotation of convective flow direction occurs repeatedly, resulting in helical vortex flows in autoclave (Fig. 5(d)). Driven by the helical flowing force of vortex flows, Ni and Co plates are assembled to radial morphology. Repeatedly helical assembly of Ni and Co plates leads to flower-like architectures (Fig. 5(e)). The existence of large amount of bubbles (Fig. 1 and Fig. 2) confirms the important role of bubbles collapse upon flower-like assembly of Ni-Co architectures.

Fluid flow is the common occurrence during hydrothermal reactions. Li et al. [11, 12] have investigated the convective flow in hydrothermal autoclaves. Numerical simulation of natural convection in autoclave has been performed by Yoshio et al [5]. Furthermore, bubbles usually appear in the boiling solution of hydrothermal reactions, and the high energy water jets and shock waves resulted from bubble collapse have been reported [7, 13, 14]. However, combination of convective flows and water jets to form vortex flows during hydrothermal reactions has not been found, elsewhere.

From vortex generator to chirality-specific lift forces, the interesting vortex flows are becoming newly hot topics in scientific research [1-4]. Compared with some exterior forces (electric and magnetic types) [15, 16] and interior forces (Van De Waals) [17], the vortex flows will give some new ideas to drive the assembly of micro/nano-structures with desired dimension and morphology.

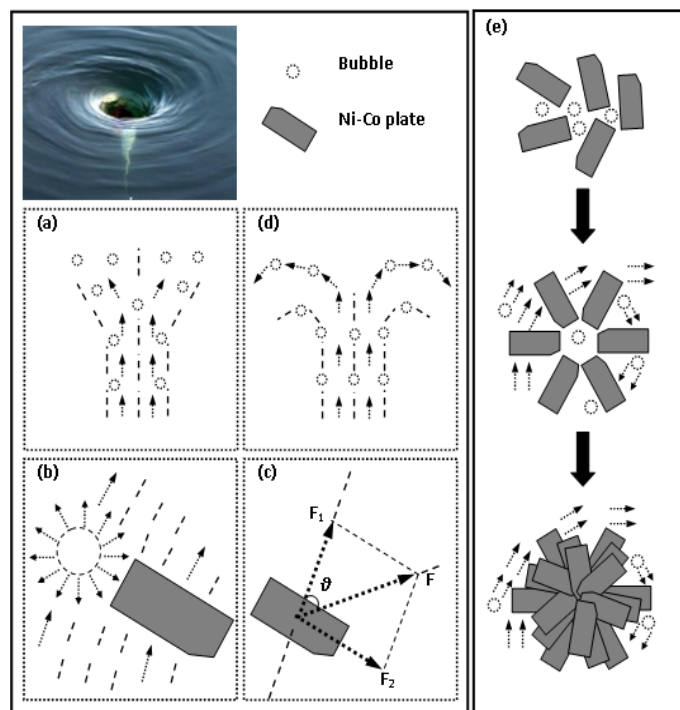


Fig. 5: Schematic assembly illustration of flower-like Ni-Co architectures. The inset of Fig. 5 is a photograph of vortex in water.

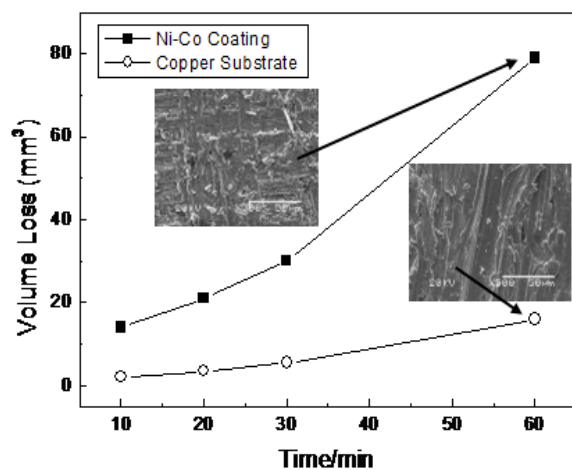


Fig. 6: Volume loss against sliding time during wear tests of copper substrate and Ni-Co coating. The insets of Fig. 6 are SEM worn morphologies of copper substrate and Ni-Co coating after 60 minutes wear tests.

3.2 Wear Properties of Flower-like Ni-Co Coating

Because of the low hardness, copper and its alloy are prone to plastic deformation under wear tests, which resulted in adhesive wear [18]. Wear resistance improvement have been reported by the deposition of hard coatings on copper. After 973 K treatment under argon atmosphere, a high microhardness of 506 HV from Ni-Co coating is achieved, about 5.5 times of copper substrate (92 HV). In addition, flower-like microstructures demonstrated good wear properties [19].

As a result, the wear property of copper substrate is obviously improved by deposition of flower-like Ni-Co coating. After 60 min wear tests, the volume loss of Ni-Co coating is 20.4 % of gray cast iron, as shown in Fig. 6. Compared with copper substrate, the flower-like Ni-Co coating exhibits much smoother worn surface, confirming the improved adhesive wear than copper substrate.

4. CONCLUSION

- 1) Ni-Co coating with flower-like morphology was deposited on copper substrate by a hydrothermal approach.
- 2) During hydrothermal reactions, interaction of the convective flows and water jets resulted in vortex flows. Driven by the helical flowing force of vortex flows, helical assembly of Ni and Co plates was performed, leading to flower-like Ni-Co architectures.
- 3) After 973 K treatment under argon atmosphere, a high micro harness of 506 HV from Ni-Co coating is achieved, about 5.5 times of copper substrate (92 HV). During sliding wear tests, the volume loss of Ni-Co coating was 20.4 % of copper substrate, obviously increasing the wear properties of copper substrate.

ACKNOWLEDGEMENT

This work was financially supported by the Natural Science Foundation of China (51402035) and the Project of Liaoning Department of Education from China (990790).

REFERENCE

- [1] F.G. Mahmood, S. Meisam, Improving vortex tube performance based on vortex generator design, *Energy* 72 (2014) 492-500. <http://www.sciencedirect.com/science/article/pii/S0360544214006380>
- [2] P. Aditya, R.V. Vivek, Flow in vortex diodes, *Chem. Eng. Res. Des.* 102 (2015) 274-285. <http://www.cherd.ichemejournals.com/article/S0263-8762%2815%2900189-6/fulltext>
- [3] T. Meuel, Y. L. Xiong, P. Fischer, C. H. Bruneau, M. Bessafi, H. Kellay, Intensity of vortices: from soap bubbles to hurricanes, *Sci. Rep.* 3 (2013) 3455.

<https://www.researchgate.net/publication/259321245>

[4] T.M. Hermans, K.J.M. Bishop, P.S. Stewart, S.H. Davis, B.A. Grzybowski, Vortex flows impart chirality-specific lift forces, *Nat. Commun.* 6 (2015) 5640.

<http://www.nature.com/ncomms/2015/150112/ncomms6640/abs/ncomms6640.html>

[5] M. Yoshio, S. Akira, M. Yutaka, Y. Chiaki, T. Takao, Numerical simulation of natural convection heat transfer in a ZnO single-crystal growth hydrothermal autoclave-Effects of fluid properties, *J. Cryst. Growth* 311 (2009) 675-679.

<http://www.sciencedirect.com/science/article/pii/S002202480800907X>

[6] Y. Zhang, F. Liu, Conversion of graphite to carbon nanotubes (CNTs) in gray cast iron and their wear properties, *J. Phys. Chem. Solid*, being revised.

<http://www.mdpi.com/2079-4991/5/1/90/pdf>

[7] J.G. Tang, C.Q. Yan, L.C. Sun, A study visualizing the collapse of vapor bubbles in a subcooled pool, *Inter. J. Heat Mass Trans.* 88 (2015) 597-608.

<http://www.sciencedirect.com/science/article/pii/S0017931015004603>

[8] F. Liu, Y. Zhang, In-situ growth of carbon nanotubes from Ni-based coatings and their wear properties, *Diamond Relat. Mater.* 25 (2012) 144-154.

<https://www.researchgate.net/publication/257369410>

[9] F. Liu, Y. Zhang, Hydrothermal growth of Ni-based coatings on copper substrates, *Inter. J. Miner. Metall. Mater.* 19 (2012) 259-265.

<http://link.springer.com/article/10.1007%2Fs12613-012-0548-8>

[10] H.L. Cao, X.F. Qian, C. Wang, X.D. Ma, J. Yin, Z.K. Zhu, High symmetric 18-facet polyhedron nanocrystals of Cu_7S_4 with a hollow nanocage, *J. Amer. Chem. Soc.* 127 (2005) 16024-16025.

<http://pubs.acs.org/doi/abs/10.1021/ja055265y>

[11] H.M. Li, E.A. Evans, G.X. Wang, Flow of solution in hydrothermal autoclaves with various aspect ratios, *J. Cryst. Growth* 256 (2003) 146-155.

<http://www.sciencedirect.com/science/article/pii/S0022024803013009>

[12] H.M. Li, G.X. Wang, E.A. Evans, Three-dimensional flow of solution in an industry-size hydrothermal autoclave subjected to non-uniform heating-effects of a baffle on flow and temperature separation, *J. Cryst. Growth* 271 (2004) 257-267.

<http://www.sciencedirect.com/science/article/pii/S0022024804009030>

[13] B. Han, Y.X. Pan, Y.L. Xue, J. Chen, Z.H. Shen, J. Lu, X.W. Ni, Mechanical effects of laser-induced cavitation bubble on different geometrical confinements for laser propulsion in water, *Opt. Lasers Eng.* 49 (2011) 428-433.

[14] M. Philippe, H. Sascha, A bubble-driven microfluidic transport element for bioengineering, *PNAS* 29 (2004) 9523-9527.

[15] F.D. Ma, S.J. Wang, L. Smith, N. Wu, Two-dimensional assembly of symmetric colloidal dimers under electric fields, *Adv. Funct. Mater.* 22 (2012) 4334-4343.

[16] P. Kinnunen, B.H. McNaughton, T. Albertson, I. Sinn, S. Mofakham, R. Elbez, D.W. Newton, A. Hunt, R. Kopelman, Self-assembled magnetic bead biosensor for measuring bacterial growth and antimicrobial susceptibility testing, *Small* 8 (2012) 2477-2482.

[17] W.Q. Lv, W.D. He, X.N. Wang, Y.H. Niu, H.Q. Cao, J.H. Dickerson, Z.G. Wang. Understanding the oriented-attachment growth of nanocrystals from an energy point of view: a review. *Nanoscale* 6 (2014) 2531-2547.

[18] M.R. Bateni, F. Ashrafizadeh, J.A. Szpunar, R.A.L. Drew, Improving the tribological behavior of copper through novel Ti-Cu intermetallic coatings. *Wear* 253 (2002) 626-639.

[19] G.G. Tang, J. Zhang, C.C. Liu, D. Zhang, Y.Q. Wang, H. Tang, C.S. Li, Synthesis and tribological properties of flower-like MoS_2 microspheres, *Ceram. Inter.* 40 (2014) 11575-11580.